THE JOURNAL OF THE ACOUSTICAL SOCIETY OF KOREA VOL.25, NO.3E 2006. 9 pp. 115~122

Bistatic Scattering from a Hemi-Spherically Capped Cylinder

Park, Sanghyun* La, Hyoungsul* Cho, Sungho* Oh, Taekhwan* Kim, Youngshin* Lee Changwon* Na, Jungyul*
*Department of Earth & Marine Sciences, Hanyang University
(Received September 6 2006; Accepted September 18 2006)

Abstract

The bistatic scattering of an incident wave by a hemi-spherically capped cylinder is of particular interest because it has rarely been studied until the present day. The configuration of a hemi-spherically capped cylinder is similar to naval underwater weapons (submarines, mines, torpedos, etc.), but which is not exactly the same. This paper describes a novel laboratory experiment aimed at direct measurement of bistatic scattering by a hemi-spherically capped cylinder. Bistatic scattering by a hemi-spherically capped cylinder was measured in an acoustic water tank (5m long, 5m wide, 5m deep) using a high frequency projector (120kHz) and hydrophone. Measurements of monostatic scattering were also made under the same conditions. The bistatic scattering pattern by a hemi-spherically capped cylinder was measured against the incident angles (0°, 15°, 20°, 30°, 45°, 60°, 90°) in order to verify various scattering pattern characteristics by the change of incident angle. The results indicate that the bistatic scattering TS at a wide scattering angle is much stronger than the monostatic scattering TS. In bistatic scattering, the forward scattering TS is significantly stronger than the backward scattering TS, and the forward scattering pattern is also broader. In case of seven incident angles, the maximum value of forward scattering TS is about 14dB stronger than that of backward scattering TS. It is also found that forward scattering varies with the incident angle of sound to a much less extent than backscattering, and it is not seriously affected by the incident angle. These features could be the advantages of using forward scattering for detecting underwater targets at long range and increasing detection area and probability.

Keywords: *Bistatic scattering, Monostatic scattering, Forward scattering, Backward scattering, Bistatic angle, Target strength, Hemi-spherically capped cylinder*

I. Introduction

Sound scattering by cylinder has been a subject of general interest in underwater acoustics over the past years, since it can be used to model scattering by a number of underwater targets. Many theoretical and experimental studies of acoustic scattering from cylinders have been performed until the present day.

Faran (1951) and Barnard and McKinney (1961) investigated the distribution in angle of sound scattered in water by solid and air-filled cylinders. Flax (1966) proposed the mathematical analysis for the scattered far-field pressure that results from the illumination of an infinite aluminum cylinder by a plane acoustic wave, whose propagation direction makes an arbitrary angle with the normal to the cylinder axis. Doolittle and Ü berall (1966) stated the general results for the acoustic- and elastic-wave field that are generated by the impact of a plane sound wave upon an elastic cylindrical shell embedded in a fluid and enclosing another fluid. Dickey (1979) explained acoustic scattering from an infinite elastic cylinder in a fluid in terms of creeping and through waves. He developed a new theory by applying the Sommerfeld-Watson transformation to the normal mode solution. Stanton (1988-1989) developed a theoretical solution for the scattering of an incident plane wave by a fluid finite and infinite circular cylinder for all frequencies. He also developed the

Corresponding author: Sanghyun Park (p3ctacco@hanmail.net)
Dept. of Earth & Marine Sciences, Hanyang University 1271 Sa-1-dong, Ansan, Sangrok-gu, Gyeonggi-do 426-791, Korea

bistatic scattering solution to restricted geometries where the incident waves are normal or near normal to the axis of the cylinder. In addition, he developed a general solution for the scattering of sound by deformed cylinders of finite length. Clay (1991) developed low spatial resolution acoustic scattering models to model scattering by objects that are less ideal than perfect cylinders. Morse and Marston (1998) interpreted impulse response backscattering measurements for the scattering of obliquely incident plane waves by air-filled finite cylindrical shells immersed in water. Similar features were present in approximate calculations for finite cylindrical shells based on full elasticity theory and the Kirchhoff diffraction integral. As shown in the above studies, most of these studies employed monostatic scattering for horizontal and vertical cylinders. Some involved bistatic scattering for vertical cylinders in cases of restricted normal incidents. The configuration of most cylinders was generally flat at the ends. Some cases are about deformed cylinders. The study of scattering of deformed cylinders was very restricted. However, many underwater weapons such as submarines, mines, and torpedos are similar to the configuration of hemi-spherically capped cylinders. To describe the scattering of sound by naval underwater weapons in an exact manner is either impossible or extremely difficult; thus we used the configuration of the hemi-spherically capped cylinder. The configuration of the hemi-spherically capped cylinder is constituted by a cylindrical shell bounded by two hemispherical shells. The studied object is made of stainless steel. It has an external radius of 5cm and its total length is 30cm. In consideration of the frequency region of this study, this object is a geometrical scatterer because ka equals 25.9, where k is the wave number in water and a is the radius of the cylinder. This reflects a condition of detecting target in a real underwater environment to some extent. Recently, the self noise of submarines has decreased with the use of quieting technology as well as the advent of air independent propulsion. Such developments have rendered all but the most sophisticated passive sonars ineffective and made detection range using passive sonar systems smaller. As a result, interest in active sonar has been renewed in an effort to counter quieter submarines. Therefore, the dependence of active sonar systems in antisubmarine operations is presently higher. In consideration of this circumstance, we performed a new study of bistatic scattering for hemi-spherically capped cylinders in order to search for a new possibility of detecting underwater targets at a long range and increasing the detection area and probability of detection. In this paper, we describe a laboratory experiment designed to measure the bistatic scattering of the hemi-spherically capped cylinder and present some new results. These results clearly indicate that forward scattering is significantly stronger than backward scattering. In addition, bistatic scattering TS at a wide scattering angle is much stronger than the monostatic scattering TS. We also investigate the variability of bistatic scattering with respect to the incident angle of sound. In consideration of possible applications of detecting underwater target with a bistatic sonar system, forward scattering was particular interest in our study.

II. Scattering Experiment

The experiments were carried out in the water tank of the Ocean Acoustic Laboratory of Hanyang University of Korea in the spring of 2006. The tank is 5m long, 5m wide and 5m deep. In consideration of effects of multi-path interference, no four sides are parallel. During the period of the experiments, the tank was filled with fresh water, and the water depth was 5m.

2.1. Description of the experiment of monostatic scattering.

Figure 1 shows the experimental geometry for the monostatic scattering measurement of the hemi-spherically capped cylinder. The carrier frequency was 120 kHz and a pulse length of 0.1ms was used to avoid multi-path signals. The beamwidth of the transducer (120 kHz) was 14°. Table 1 shows the specifications of the hemi-spherically capped cylinder and transducer (120 kHz).

The studied object was made of steel. Its thickness was 0.3mm, and it was filled with air. It had an external radius of 5cm and a total length is 30cm. In consideration of the frequency region

Material	Thickness	Inside condition
steel	0.3mm	Air-filled

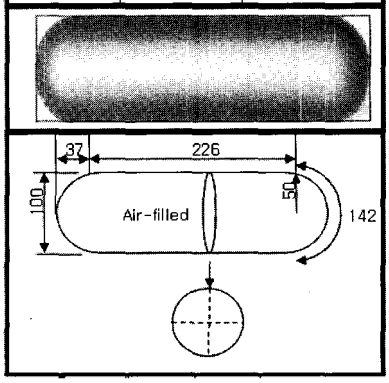

(단위 mm)

Table 1. Specification of the hemi-spherically capped cylinder and equipment.

Projector (Neptune Sonar)		Hydrophone (Reson)
Frequency	120 kHz	15 Hz ~ 480 kHz
TVR*	174.9dB	-
RVS*	-187dB	-186dB +- 3dB
Beam Width	14°	Omni-direction
Pulse Length	0.1ms	-

*TVR: Transmitted Voltage Response- *RVS: Receiving Voltage Sensitivity

of this study, the studied object was a geometrical scatterer because ka equals 25.9, where k is the wave number in water and a is the radius of the studied object.

As shown in figure 1, the incident angle is defined by the angle between the incident wave and the cylinder axis. In this experiment, the impulse monostatic setup is used and consists of sending a short pulse by a transducer of frequency 120 kHz and receiving the backscattered signal from the hemi-spherically capped cylinder using the same transducer.

According to this experimental geometry, echo wave form recordings, the hemi-spherically capped cylinder is rotated by the center point of its geometrical center from 0° to 360° at 0.88° intervals and placed next to each other. The combination of transducer directivity, object position and vertical location of the transducer (2.05m above the bottom of the water tank and 2.95m below the water's surface) eliminated interference due to multi-path signals. The range between source and scatterer is 2.15m, and it is longer than the critical range $R_c(\cong a^2/\lambda)$. Therefore, there is no near-field effect (Medwin & Clay, 1997). In the critical range equation, R_c is a critical range, a is a radius of the 120kHz transducer and λ is a wavelength in water. The scattered wave also received in the far-field $kR>>1$. Data on echo structure and target strength were recorded using an oscilloscope display while distribution-in-angle data were recorded on hard disk of a personal computer.

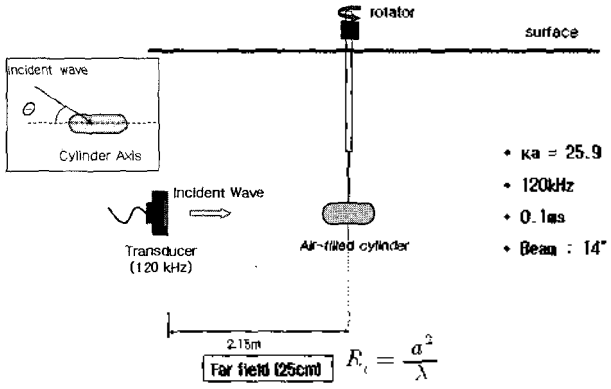

Figure 1. Monostatic experimental geometry for sound scattering measurement of the hemi-spherically capped cylinder.

2.2. Description of the experiment of bistatic scattering.

Figure 2 shows the experimental geometry for bistatic scattering measurement of The hemi-spherically capped cylinder. The carrier frequency was 120 kHz and a pulse length of 0.1ms was used to avoid the multi-path signals.

First, we set up pan and tilter parallel with the flat bottom in a water tank and attached the hemi-spherically capped cylinder above it as shown in figure 2. A projector (120 kHz) is located at a depth of 2.95m pointing to the center of the hemi-spherically capped cylinder. The hydrophone is held at a fixed distance (1m) from the hemi-spherically capped cylinder by means of a boom and rotated in plane to demonstrate the scattered field in that plane. The angular interval of the hydrophone rotation is 0.9°. The range between source and cylinder is 1.6m, and it is longer than the critical range $R_c(\cong a^2/\lambda)$. Therefore, there is no near-field effect (Medwin & Clay, 1997). In the critical range equation, R_c is a critical range, a is a radius of the projector (120kHz) and λ is a wavelength in water. The scattered wave is also received in the far-field $kR>>1$. The scattering measurements were restricted to those obtained by rotating the hydrophone through 360° in that plane.

According to the experimental geometry in figure 2, the projector (120 kHz) radiates sound to the hemi-spherically capped cylinder. The hydrophone receives the scattered signals at the same distance, turning around the geometrical center of hemi-spherically capped cylinder at 0.9° intervals and placed next to each other. We received five ping signals at 0.9° intervals for detailed analysis. We gave the delaying time 20 seconds at 0.9° intervals in order to stabilize hydrophone vibration. The combination of projector directivity, hydrophone position and vertical location of the projector (2.05m above the water tank and 2.95m below the water's surface) eliminated interference due to

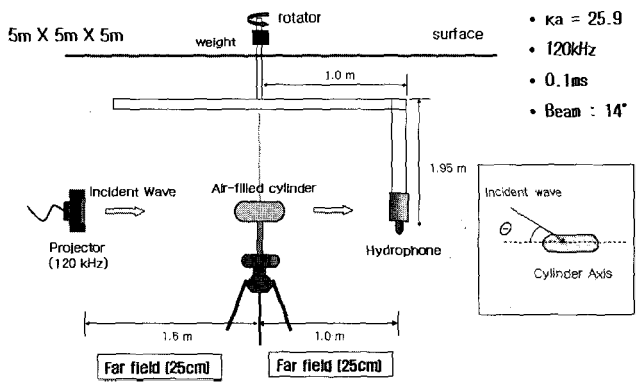

Figure 2. Bistatic experimental geometry for sound scattering measurement of the hemi-spherically capped cylinder.

multi-path signals. However, we had significant difficulty measuring bistatic scattering because the forward scattered signal arrived at the hydrophone at almost the same time as the direct path signal in some ranges. This is in contrast to measuring backscattering in which case the echo can separated be from the transmitted signal in time with a pinging technique. In order to solve this difficulty, we performed an additional experiment under the same conditions in the absence of the hemi-spherically capped cylinder. The scattered signals were monitored and recorded with the digital oscilloscope.

2.3. Data acquisition and analysis.

The incident wave was a CW pulse generated with a waveform generator (AGILENT 33120A). The signal was then amplified by a power amplifier (B&K model 2610) and sent to the projector. The digital oscilloscope monitored the voltage and current from the power amplifier. The hydrophone received the scattered signals by the hemi-spherically capped cylinder, and the signals were monitored and recorded by the digital oscilloscope.

Figure 3 shows the system block diagram of the scattering measurement experiment. The simple diagram seeks to capture how the incident signals are generated and the scattered signals are received. This system is controlled automatically by the ARRS (Auto Rotating and Receiving System) (Figure 4)

As shown in figure 4, the computer is connected to the rotator and wave generator. They are controlled by MATLAB. This system consists of a rotator, a hydrophone and a receiving system. First, the wave generator makes the signals and the projector transmits the signals. Second, the hydrophone hung at the end of the bar turns around the hemi-spherically capped cylinder and receives the scattered signal at 0.9° intervals.

Figure 5 shows the top view of the bistatic experimental geometry. Source, object and receiver are located at the same depth and in plane. As sketched in figure 5, the incident wave is directly received by the hydrophone at position ①. The scattered wave from the hemi-spherically capped cylinder is reached by the receiver along with the circle. However, the direct and scattered paths overlap at position ③ because this experiment was conducted in a very restricted space.

The most significant difficulty of measuring bistatic scattering was that the forward scattered signals arrived at the hydrophone at almost the same time as the direct path signals. Therefore, in order to solve this difficulty, we simply recorded the first signals received at the hydrophone in the absence of the hemi-spherically capped cylinder, which were the free-field signals. Then, we recorded the scattered signals with the hemi-spherically capped cylinder in the water, from which we could subtract the free-field signals. To obtain forward scattering signals, we had two experiments using the same conditions. In the two measurements (with and without hemi-spherically capped cylinder), the recorded

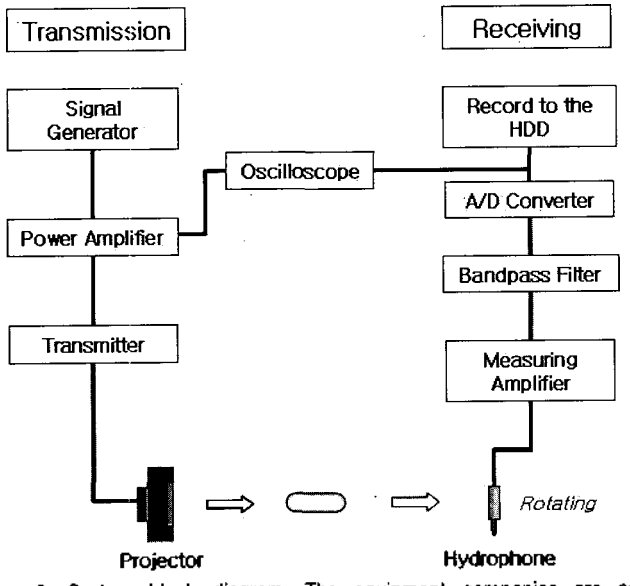

Figure 3. System block diagram. The equipment companies are as follows: Arbitrary Waveform Generator (Agilent 33120A), Power Amplifier (B & K Type 2713) and Measuring Amplifier (B & K type 2610), Bandpass Filter (K-H model 3940), A/D Converter (National Inst).

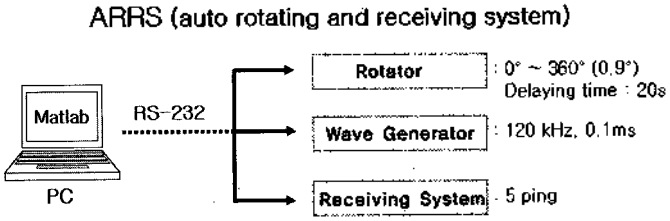

Figure 4. Auto Rotating and Receiving System (ARRS). The computer is connected to the rotator and wave generator. They are controlled by Matlab. First, the rotator rotates the hydrophone, and the wave generator makes the signals. Second, the projector transmits the signals, and the hydrophone receives the scattered signals.

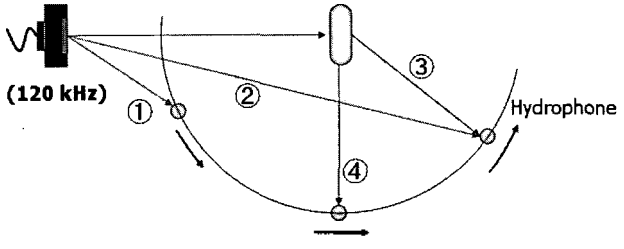

①, ② : direct wave from the source
③, ④ : scattered wave from the cylinder

Figure 5. Top view of the experimental geometry in figure 2. The numbers in circles indicate the position of the hydrophone. The dashed lines are the path of the scattered wave.

waveforms should not be affected artificially on the phase. To acquire stable signals for each measurement, we averaged over five pings and took special care to keep the hydrophone stable. The received signals were monitored and recorded with a digital oscilloscope. The digital oscilloscope can simultaneously display waveforms of up to four channels and record them on to hard disks for further analysis. Figure 6 shows an example of bistatic scattering signals from the hemi-spherically capped cylinder at 0° to 90° in case of incident angle 0°. The signals are taken to 2ms. The direct path signals from source and scattered signals from hemi-spherically capped cylinder are received around 0.4ms and 1.8ms respectively. The arrival time of the direct signals decreases from 0° to 90° and increases from 90° to 180°. However, the scattered signals always measure 1.8ms because the hydrophone turns around the hemi-spherically capped cylinder at the same distance. This shows that the experimental geometry is correct.

The measured data were used to calculate target strength values at 0.9° intervals. To calculate target strength values, we used the method of PTS (peak target strength). It is the simplest to measure the peak pressures of the incident and reflected pulses. Therefore, peak target strength is usually determined regardless of the method of measurement and the parameter normally used in active sonar equations. In bistatic sonar systems, the method of computing target strength is slightly different from that of a monostatic sonar system. The target strength (TS) in bistatic active sonar equations is given by (Cox, 1988)

$$TS = RL - SL + (TL1 + TL2) \quad (1)$$

where TS is the target strength (dB re 1μPa at 1m), SL is the source level (dB re 1μPa at 1m), TL1 is the transmission loss from source to cylinder, and TL2 is the transmission loss from cylinder to receiver (dB re 1m). In a monostatic active sonar system, transmission loss is 2TL, but in a bistatic active sonar system, it is TL1+TL2 because source and receiver are not in the same position. RL is the reverberation level (dB re 1μPa). We calculated target strength values individually at 0.9° intervals using equation (1).

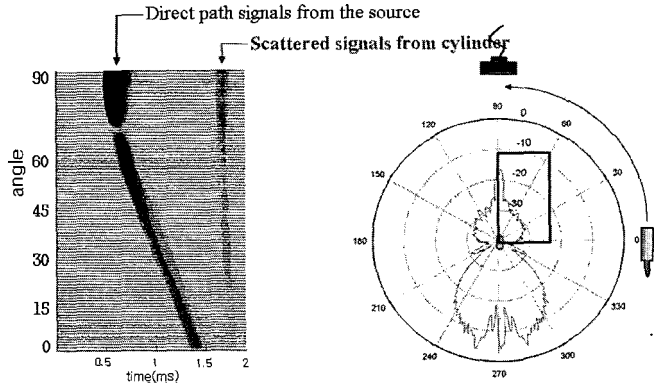

Figure 6. Direct and scattering signals of bistatic scattering from 0° to 90° in case of incident angle 0°. The direct path signals from the projector were received at the rate of around 0.4ms and 1.4ms respectively. However, scattering signals from the hemi-spherically capped cylinder were received always at the rate of around 1.8ms.

III. Experimental Results

In this experiment, we measured scattering from a hemi-spherically capped cylinder. The incident angle is defined as the angle between incident plane wave and scattered wave. Of particular interest here is the measured forward scattering, backward scattering and backscattering target strengths (TS) at various incidences, which are shown figure 7, 9 for hemi-spherically capped cylinder. Figure 7 shows a polar diagram of the distribution of backscattered acoustic energy from a hemi-spherically capped cylinder.

In figure 7, there is the maximum target strength -13.5 dB at incident angle 90°. The target strength at incident angle 90° is about 4.5 dB higher than that at incident angle 0°. Around 0°, the scattering pattern appears broader than other angles, and target strength values are larger than the others except for around 90°. As shown in figure 7, target strength fluctuates extremely when the incident angles are changed. The fluctuation appear due to constructive and destructive interference from wavelets of second sources. As a plane wave is incident on the surface of the hemi-spherically capped cylinder, the Huygens wavelets

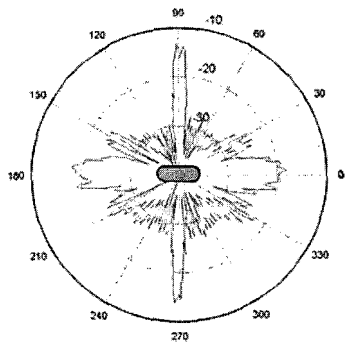

Figure 7. This is the monostatic scattering pattern from the hemi-spherically capped cylinder. This figure indicates a polar diagram of the distribution of the backscattered acoustic energy from the hemi-spherically capped cylinder. The hydrophone receives the backscattered signals at incident angle 0.88° intervals.

originating at the surface of the hemi-spherically capped cylinder go in all directions (Medwin & Clay, 1997). According to the position of hydrophone and the change of incident angles, target strength fluctuates. The results for target strength versus incident angles, obtained from the specular reflection of sound waves, are in general similar to the results predicted by the surface curvatures at the specular reflection points. The results are as expected for the specular reflected sound wave results. The measured monostatic scattering pattern was used to compare with the bistatic scattering pattern. In this monostatic scattering experiment, we verify that target strength values in a very restricted range appear higher than the others. It is a small part of the omni-directional azimuth angle. Figure 9 shows a polar diagram of the distribution in angle in the plane to the scattered acoustic energy from the horizontal hemi-spherically capped cylinder for various incident angles. It is taken at a frequency of 120 kHz with a pulse length of 0.1ms. In this experiment, the bistatic angle (β) is defined by the angle between the path from source to target and the path from target to receiver (Cox, 1989). As shown in figure 9(a), the projector (120kHz) is located at an angle of 90° and the hydrophone turns around the hemi-spherically capped cylinder from 0° to 360°. Polar diagrams indicate omni-directional scattered energy in plane from the geometrical center of the hemi-spherically capped cylinder for various incident angles. As a result, the forward scattering TS is much stronger than the backward scattering TS, and the difference increases dramatically with azimuthal angle.

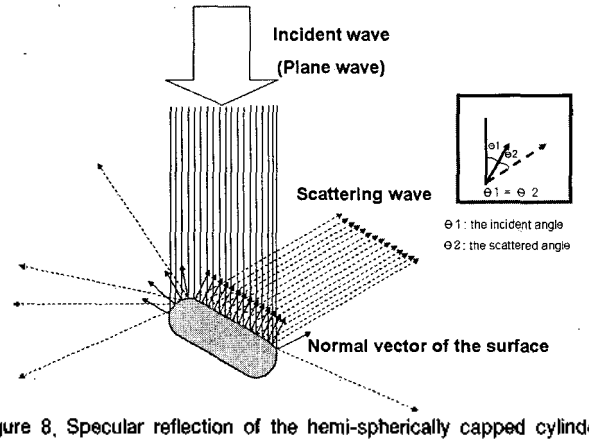

Figure 8. Specular reflection of the hemi-spherically capped cylinder in the case of an incident angle of 45° . A solid line is the incident plane wave. An arrow solid line is the normal vector of the surface of the cylinder; an arrow dotted line is the scattered wave by the surface of the hemi-spherically capped cylinder. Like the above rectangular box, the incident angle (θ 1) is the same as the scattered angle (θ 2). In the backward scattering region of bistatic scattering, the scattering pattern is generated by this specular reflection of the scattering mechanism.

The maximum forward scattering TS is about 14 dB stronger than the maximum backward scattering TS. The bistatic scattering TS at β 140°~180° is much stronger than the others. The forward scattering pattern is also much broader than the backward

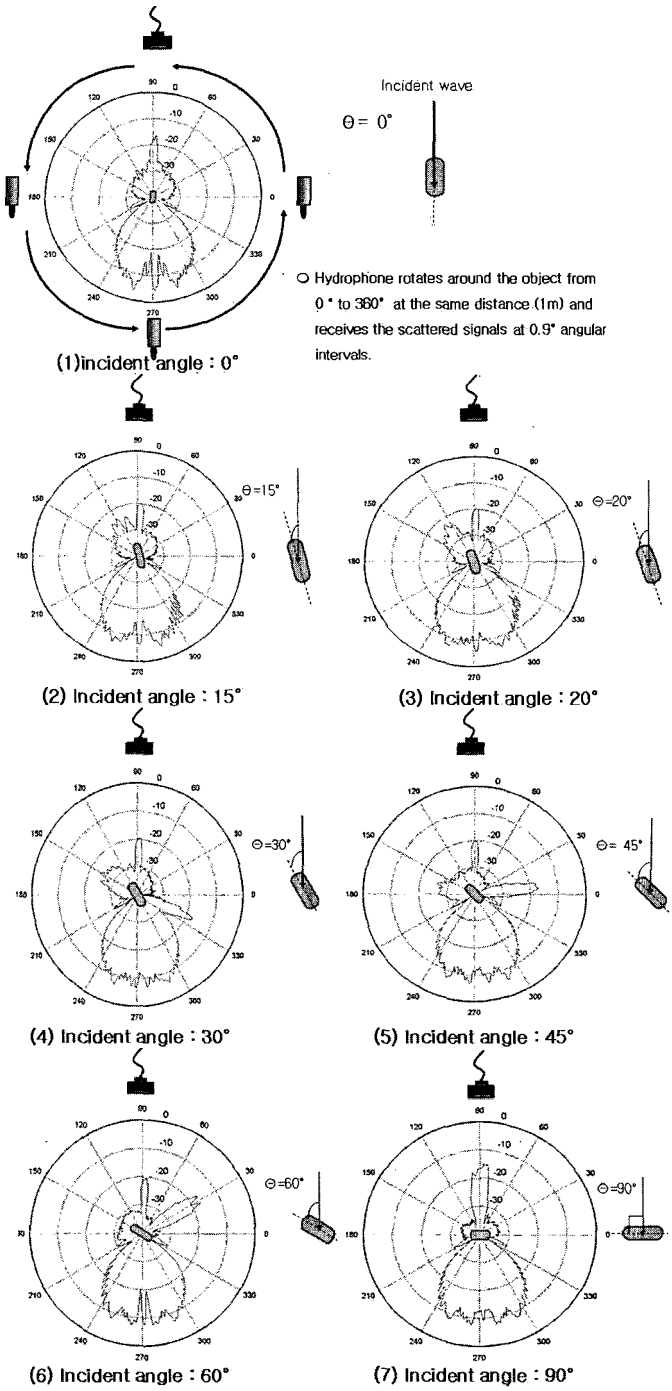

Figure 9. This is the bistatic scattering pattern from the hemi-spherically capped cylinder. This figure means a polar diagram of the distribution of scattered energy from the hemi-spherically capped cylinder at incident angles (0° , 15° , 20° , 30° , 45° , 60° , 90°). A projector is located at 90° in the polar diagram. The hydrophone turns around the hemi-spherically capped cylinder from 0° to 360° at a fixed distance (1m) and receives the scattered signals at 0.9° angular intervals.

scattering pattern. In this paper, we cannot compare experimental results with theoretical solutions because it is very difficult to demonstrate theoretical solution for the bistatic scattering of hemi-spherically capped cylinder in the forward scattering region. However, we find that the interesting aspect of the measured acoustic scattering by the deformed cylinder (hemi-spherically capped cylinder), never obtained before, is a bistatic scattering pattern with various incident angles. Therefore, figure 9 shows the measured bistatic scattering pattern (i.e., target strength versus the bistatic angle β).

Figure 8 shows the specular reflection of the scattering mechanism. In figure 8, the projector (120 kHz) radiates the incident plane wave to the hemi-spherically capped cylinder. A plane wave is an incident on the surface of the hemi-spherically capped cylinder and the incident wave is scattered at an omni-directional angle. In figure 8, a solid line is the incident plane wave, an arrow solid line is the normal vector of the surface of the hemi-spherically capped cylinder and an arrow dotted line is the scattered wave by the surface of hemi-spherically capped cylinder. As shown in figure 8, the incident angle ($\Theta 1$) is the same as the scattered angle ($\Theta 2$). In conclusion, backward scattering pattern is generated by the specular reflection of the geometrical shape of the hemi-spherically capped cylinder. Finally, comparing the bistatic scattering with the monostatic scattering, the bistatic scattering TS is overall much stronger than the monostatic scattering TS. Moreover, the forward scattering pattern is broader than the monostatic scattering pattern. This shows that bistatic scattering can offer a new possibility of detecting an underwater target at a long distance and increasing the detection probability and area.

IV. Discussion

In this paper, we found the result of the bistatic scattering pattern from the hemi-spherically capped cylinder for various incident angles through an experiment of scattering measurement. The bistatic scattering pattern is very different from the monostatic scattering pattern. The bistatic scattering TS is stronger than the monostatic scattering TS. In the bistatic scattering, the forward scattering pattern is broader than the backward scattering pattern and the forward scattering TS is much stronger. However, we cannot compare experimental data with theoretical solutions because it is very difficult to demonstrate the theoretical solution and theoretical studies almost have not done until now. The most significant difficulty of measuring bistatic scattering was that the forward scattered signals arrived at the hydrophone at almost the same time as the direct path signals. Therefore, in order to solve this difficulty, we simply recorded the signals received at the hydrophone first in the absence of the hemi-spherically capped cylinder, which were the free-field signals. Then, we recorded the scattered signals with the hemi-spherically capped cylinder in the water, from which we could subtract the free-field signals. However, in the future, we must minimize the overlap part of the direct and scattering signals in the forward scattering region by moving past the restricted experimental condition for more accurate analysis. This must be done in conjunction with the theoretical study of bistatic scattering. Our experimental results must certainly be verified by theoretical solutions in the future.

V. Summary and Conclusions

An experimental study of bistatic scattering by a hemi-spherically capped cylinder was performed. This paper shows the experimental results of the bistatic scattering pattern from a hemi-spherically capped cylinder. The goal of this paper was to understand the scattered energy distributions in plane from an air-filled hemi-spherically capped cylinder with various incident angles. Experiments were conducted to measure the scattered energy as a function of azimuth angle for various incident angles. The bistatic scattering pattern was measured in plane from a hemi-spherically capped cylinder. First, a plane wave is incident on the hemi-spherically capped cylinder with various incident angles. Second, the hydrophone turns around the cylinder at a fixed distance and receives scattered signals in plane. We cannot compare experimental results with theoretical solutions in the forward scattering region because it is very difficult to demonstrate theoretical solution, and very few theoretical studies have been performed until now. However, we verify that the forward scattering TS is much stronger than the backward scattering and backscattering (monostatic scattering) TS. Moreover, the forward scattering pattern is much broader than backward scattering. The forward scattering pattern at various incident angles is very similar to each other and is not seriously affected by incident angle. In this paper, the most interesting aspect of the measured acoustic scattering by

hemi-spherically capped cylinder, never obtained before, was the bistatic scattering pattern. Although practical techniques of the bistatic sonar have yet to be developed, we believe that this experimental study provides a more complete understanding of sound bistatic scattering by a hemi-spherically capped cylinder and lays the foundations for future development of related technology. Finally, the primary conclusion of this study shows that bistatic scattering can offer a new possibility of detecting underwater targets at a longer range and increasing the detection area and probability of detection in the future

References

1. James J. Faran, JR, "Sound Scattering by Solid Cylinders and Spheres," J. Acoust. Soc. Am., 23 405-418, 1951.
2. G. R. Barnard and C. M. McKinney, "Scattering of acoustic energy by solid and air-filled cylinders in water," J. Acoust. Soc. Am., 33 226-238, 1961
3. Doolittle, R. D. and H Überall, "Sound Scattering by Elastic Cylindrical Shells," J. Acoust. Soc. Am., 39 272-275 (1966).
4. Lawrence Flax, "Scattering of an obliquely incident acoustic wave by an infinite cylinder," J. Acoust. Soc. Am., 68 1832-1835, 1966.
5. J. W. Dickey, "Acoustic high-frequency scattering by elastic cylinders," J. Acoust. Soc. Am., 66 (1) 275-283, 1979.
6. T.K Stanton, "Sound scattering by cylinders of finite length I. Fuild cylinders," J. Acoust. Soc. Am., 83 5563, 1988.
7. T.K Stanton, "Sound scattering by cylinders of finite length II. Elastic cylinders," J. Acoust. Soc. Am., 83 (1) 64-67, 1988.
8. T.K Stanton, "Sound scattering by cylinders of finite length III. Deformed cylinders," J. Acoust. Soc. Am., 83 (2) 691-705, 1989
9. C. S. Clay, "Low-resolution acoustic scattering models: Fluid-filled cylinders and fish with swim bladders," J. Acoust. Soc. Am., 89 (5) 2168-2179, 1991.
10. Scot F. Morse and Philip L. Marston, "High-frequency backscattering enhancements by thick finite cylindrical shells in water at oblique incidence; Experiments, interpretation, and calculations," J. Acoust. Soc. Am., 103 (2) 785-794, 1998.
11. H. Medwin, and C. S. Clay, Fundamentals of Acoustical Oceanography, Academic Press, New York, 1997.
12. Henry Cox, Fundamentals of bistatic active sonar, Kluwer Academic Publishers, Arlington, 1989

[Profile]

•Park, Sanghyun

2000. 3: Dept. of Management Science, Naval Academic, Korea (BS)
2005. 3~present: Dept. of Earth & Marine Science, Seoul, Korea (MS; Underwater Acoustics)
※ Research field: acoustic target strength(Hemi-spherically capped cylinder), scattering pattern measurement.

•La, Hyoungsul

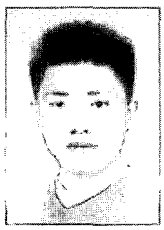

The Journal of the Acoustical Society of Korea, Vol. 24, No. 2, 2005.

•Cho, Sungho

2005. 2: Dept. of Earth & Marine Science, Seoul, Korea (BS)
2005. 3~present: Dept. of Earth & Marine Science, Seoul, Korea (MS; Underwater Acoustics)

•Oh, Taekhwan

The Journal of the Acoustical Society of Korea, Vol. 24, No. 6, 2005.

•Kim, Youngshin

1997. 2: Dept. of Earth & Marine Science, Seoul, Korea (BS)
1997. 3~2004. 8: Dept. of Earth & Marine Science, Seoul, Korea (MS; Underwater Acoustics)
2004. 9~present: Dept. of Earth & Marine Science, Seoul, Korea (Ph.D; Underwater Acoustics)

•Lee Changwon

1999. 2: Dept. of Earth & Marine Science, Seoul, Korea (BS)
1999. 3~2002. 2: Dept. of Earth & Marine Science, Seoul, Korea (MS; Underwater Acoustics)
2003. 8~present: Dept. of Earth & Marine Science, Seoul, Korea (Ph.D; Underwater Acoustics)

•Jungyul Na

The Journal of the Acoustical Society of Korea, Vol. 23, No. 4, 2004.